

Exploring Transition from Stability to Chaos through Random Matrices

Roberto da Silva, Sandra Prado
Instituto de Física, Universidade Federal do Rio Grande do Sul

This study explores the application of random matrices to track chaotic dynamics within the Chirikov standard map. Our findings highlight the potential of matrices exhibiting Wishart-like characteristics, combined with statistical insights from their eigenvalue density, as a promising avenue for chaos monitoring. Inspired by a technique originally designed for detecting phase transitions in spin systems, we successfully adapt and apply it to identify analogous transformative patterns in the context of the Chirikov standard map. Leveraging the precision previously demonstrated in localizing critical points within magnetic systems in our prior research, our method accurately pinpoints the Chirikov resonance-overlap criterion for the chaos boundary at $K \approx 2.43$, reinforcing its effectiveness.

I. INTRODUCTION

Chaotic behavior plays a crucial role in contemporary physics [1], as the comprehension of non-determinism under initial conditions arises in various contexts, including the stabilization of seemingly simple mechanical systems, such as the inverted pendulum [2, 3].

The identification of chaos in specific Hamiltonian systems can be accomplished using traditional methods; however, there is room for the development of various alternatives. In contrast, the theory of random matrices has provided a robust and potent toolkit for describing several aspects of physical phenomena. This journey began with Wigner's pioneering work, which explained the intricate distribution of energies in heavy nuclei [4, 5]. Subsequently, Dyson, displaying remarkable foresight, discerned that the joint distribution of eigenvalues in symmetric random matrices, characterized by well-behaved matrix entries, behaves analogously to a Coulomb gas of charged particles exhibiting logarithmic repulsion [6].

In recent times, the authors of this study have recognized the potential of a class of matrices known as Wishart-like matrices [7], demonstrating their successful application in characterizing the critical behavior of spin systems. This insight is revealed through the analysis of the spectra of these matrices, as presented in our prior works [8–10].

The concept revolves around considering a specified number of time evolutions of magnetization, acquired through a particular dynamics (e.g., Metropolis), as columns within matrices [8]. These rectangular matrices are then transformed into square matrices by multiplying the matrix by its transpose, wherein the eigenvalues of these matrices offer insights into the correlations among the time series data. Notably, phase transitions are associated with deviations from the Marchenko-Pastur eigenvalue density, which typically characterizes uncorrelated time series data [11].

This paper aims to investigate the relationship between time series generated through simple map iterations, exhibiting chaotic behavior, and the spectral properties of Wishart-like matrices constructed from these series. In essence, we seek to determine whether chaotic behavior is discernible in these spectra, thereby offering an alternative avenue for the study of chaotic phenomena.

To accomplish this objective in our study, we have opted for the Chirikov map iteration method [12]. This method's origins trace back to a particle subjected to the influence of a kicked potential, governed by a time-dependent Hamiltonian:

$$\mathcal{H}(q, p, t) = \frac{p^2}{2m} + K \cos q \sum_{n=0}^{\infty} \delta(t - n) . \quad (1)$$

The dynamics consist of a sequence of free propagations interspersed with periodic kicks. The Hamiltonian equations yield:

$$\frac{dq}{dt} = \frac{\partial \mathcal{H}}{\partial p} = \frac{p}{m} \quad (2)$$

$$\frac{dp}{dt} = -\frac{\partial \mathcal{H}}{\partial q} = K \sin q \sum_{n=0}^{\infty} \delta(t - n)$$

Hence, the Chirikov standard map, which preserves the area in the phase space of the two canonical dynamical variables (q and p), is defined as follows:

$$\begin{aligned} p_{n+1} &= p_n + K \sin q_n \\ q_{n+1} &= q_n + p_n. \end{aligned} \tag{3}$$

We consider a unitary mass, $m = 1$, for which the dynamics can be visualized either within a cylinder by taking $q \bmod 2\pi$ or on a torus. In the latter scenario, we take $q \bmod 2\pi$ and $p \bmod 2\pi$.

From this interaction, we construct square matrices and monitor their spectra as a function of K . Our findings indicate that the theoretical conjectures for the chaotic boundaries appear to be reflected in the minimal and maximal values of eigenvalue fluctuations (moments of eigenvalue density).

In next section we present a brief tutorial about random matrices with particular interest in Wishart-like matrices. We will show how the method worked to find the critical behavior of Ising model and why it must works to find the chaotic behavior of the Chirikov map. In section

In the upcoming section, we offer a concise tutorial on random matrices, with a dedicated emphasis on Wishart-like matrices. We will delve into how this method has effectively revealed the critical behavior of the Ising model and why we hold the expectation that it will similarly shed light on the chaotic behavior of the Chirikov map. Following that, in Section III, we present our primary findings. Lastly, we draw our study to a close by summarizing our conclusions in Section IV.

II. WISHART-LIKE RANDOM MATRICES: AN EXPLORATION OF THEIR NOVEL APPLICATION IN STATISTICAL MECHANICS

The foundation of random matrices theory can be traced back to its inception within the realm of nuclear physics, as E. Wigner [4, 5] pioneered its development to describe the intricate energy levels of heavy nuclei. Wigner achieved this by representing the nucleus's Hamiltonian using matrices with randomly distributed entries

When considering symmetric matrices ($h_{ij} = h_{ji}$) with well-behaved entries, i.e., entries following a probability density function $f(h)$ such that

$$\int_{-\infty}^{\infty} dh_{ij} f(h_{ij}) h_{ij} < \infty, \tag{4}$$

$$\int_{-\infty}^{\infty} dh_{ij} f(h_{ij}) h_{ij}^2 < \infty$$

of a matrix H , with dimensions $N \times N$, featuring independent entries, and thus characterized by a joint distribution given as:

$$\Pr\left(\prod_{i < j} h_{ij}\right) = \prod_{i < j} f(h_{ij}). \tag{5}$$

This leads to a joint eigenvalue distribution $P(\lambda_1, \dots, \lambda_N)$, and its eigenvalue density is defined as follows:

$$\sigma(\lambda) = \int_{-\infty}^{\infty} \dots \int_{-\infty}^{\infty} P(\lambda, \lambda_2, \lambda_3, \dots, \lambda_N), \tag{6}$$

which, under the earlier-stated conditions for the matrix entries h_{ji} , is universally characterized by the semi-circle law [13, 14]:

$$\sigma(\lambda) = \begin{cases} \frac{1}{\pi} \sqrt{2N - \lambda^2} & \text{if } \lambda^2 < 2N \\ 0 & \text{if } \lambda^2 \geq 2N \end{cases} \tag{7}$$

In the particular context where $f(h_{ij}) = \frac{e^{-h_{ij}^2/2}}{\sqrt{2\pi}}$, we can establish the Boltzmann weight as follows:

$$P(\lambda_1, \dots, \lambda_N) = C_N \exp \left[-\frac{1}{2} \sum_{i=1}^N \lambda_i^2 + \sum_{i < j} \ln |\lambda_i - \lambda_j| \right],$$

where $C_N^{-1} = \int_0^\infty \dots \int_0^\infty d\lambda_1 \dots d\lambda_N \exp[-\mathcal{H}(\lambda_1 \dots \lambda_N)]$ denotes the inverse of the normalization constant for a Coulomb gas with the Hamiltonian:

$$\mathcal{H}(\lambda_1 \dots \lambda_N) = \frac{1}{2} \sum_{i=1}^N \lambda_i^2 - \sum_{i<j} \ln |\lambda_i - \lambda_j|$$

operating at an inverse temperature $\beta^{-1} = 1$. The final term exhibits logarithmic repulsion, akin to the conventional Wigner/Dyson ensembles, as elucidated by Dyson [6]. Simultaneously, the first term exerts an attractive influence. In the context of hermitian or symplectic entries, as elucidated by Mehta [13], the outcome remains comparable. Specifically, it yields $P(\lambda_1, \dots, \lambda_N) = C_N^\beta \exp(-\beta\mathcal{H})$, with β taking values of 2 and 4, resulting in a consistently shared eigenvalue density 7.

Despite the apparent analogy, there is no immediate bridge between the thermodynamics of a real-world system and the fluctuations observed in random matrices generated from data originating from that very system. However, when one delves deeper into the quest for correlations, this bridge starts to materialize. Its comprehension holds the key to unlocking insights into phase transitions and critical phenomena within Thermostatistics.

It's worth noting that nearly three decades before Wigner and Dyson's groundbreaking work, Wishart [7] pioneered the analysis of correlated time series. Rather than resorting to Gaussian or Unitary ensembles, he delved into the realm of the Wishart ensemble. This ensemble primarily deals with random correlation matrices, distinguishing it from the conventional approaches of his contemporaries.

In recent contributions [8], we have explored this avenue by introducing the magnetization matrix element m_{ij} representing the magnetization of the j th time series at the i th Monte Carlo (MC) step within a system of $N = L^d$ spins. For simplicity in our investigations, we adopted $d = 2$, the minimum dimension where a phase transition occurs in the simple Ising model. Additionally, we delved into the mean-field Ising model [9], maintaining the same total number of spins.

Here, $i = 1, \dots, N_{MC}$, and $j = 1, \dots, N_{sample}$. Consequently, the magnetization matrix M assumes dimensions $N_{MC} \times N_{sample}$. To scrutinize spectral properties more effectively, we propose an intriguing alternative: rather than analyzing M , we turn our attention to the square matrix of dimensions $N_{sample} \times N_{sample}$:

$$G = \frac{1}{N_{MC}} M^T M ,$$

resulting in $G_{ij} = \frac{1}{N_{MC}} \sum_{k=1}^{N_{MC}} m_{ki} m_{kj}$ a matrix well-known as the Wishart matrix [7]. At this juncture, rather than continuing with m_{ij} it becomes more advantageous to operate with the matrix M^* , whose elements are defined through the customary variables:

$$m_{ij}^* = \frac{m_{ij} - \langle m_j \rangle}{\sqrt{\langle m_j^2 \rangle - \langle m_j \rangle^2}},$$

where:

$$\langle m_j^k \rangle = \frac{1}{N_{MC}} \sum_{i=1}^{N_{MC}} m_{ij}^k .$$

Thereby:

$$\begin{aligned} G_{ij}^* &= \frac{1}{N_{MC}} \sum_{k=1}^{N_{MC}} \frac{m_{ki} - \langle m_i \rangle}{\sqrt{\langle m_i^2 \rangle - \langle m_i \rangle^2}} \frac{m_{kj} - \langle m_j \rangle}{\sqrt{\langle m_j^2 \rangle - \langle m_j \rangle^2}} \\ &= \frac{\langle m_i m_j \rangle - \langle m_i \rangle \langle m_j \rangle}{\sigma_i \sigma_j} \end{aligned} \quad (8)$$

where $\langle m_i m_j \rangle = \frac{1}{N_{MC}} \sum_{k=1}^{N_{MC}} m_{ki} m_{kj}$ and $\sigma_i = \sqrt{\langle m_i^2 \rangle - \langle m_i \rangle^2}$. Analytically, when m_{ij}^* are uncorrelated random variables, the joint distribution of eigenvalues can be described by the Boltzmann weight [15, 16]:

$$P(\lambda_1, \dots, \lambda_{N_{sample}}) = C_{N_{sample}} \exp\left[-\frac{N_{MC}^2}{2N_{sample}} \sum_{i=1}^{N_{sample}} \lambda_i - \frac{1}{2} \sum_{i=1}^{N_{sample}} \ln \lambda_i + \sum_{i<j} \ln |\lambda_i - \lambda_j|\right]$$

where $C_{N_{sample}}^{-1} = \int_0^\infty \dots \int_0^\infty d\lambda_1 \dots d\lambda_{N_{sample}} \exp[-\mathcal{H}(\lambda_1 \dots \lambda_{N_{sample}})]$, and this corresponds to the Hamiltonian:

$$\mathcal{H}(\lambda_1 \dots \lambda_{N_{sample}}) = \frac{N_{MC}^2}{2N_{sample}} \sum_{i=1}^{N_{sample}} \lambda_i + \frac{1}{2} \sum_{i=1}^{N_{sample}} \ln \lambda_i - \sum_{i < j} \ln |\lambda_i - \lambda_j|.$$

In this case, the density of eigenvalues $\rho(\lambda)$ of the matrix $G^* = \frac{1}{N_{MC}} M^{*T} M^*$ follows the well-known Marcenko-Pastur distribution [11], which for our case we write as:

$$\rho(\lambda) = \begin{cases} \frac{N_{MC}}{2\pi N_{sample}} \frac{\sqrt{(\lambda - \lambda_-)(\lambda_+ - \lambda)}}{\lambda} & \text{if } \lambda_- \leq \lambda \leq \lambda_+ \\ 0 & \text{otherwise,} \end{cases} \quad (9)$$

where $\lambda_{\pm} = 1 + \frac{N_{sample}}{N_{MC}} \pm 2\sqrt{\frac{N_{sample}}{N_{MC}}}$.

In our studies [8, 9], we examined the behavior of $\rho_{\text{numerical}}(\lambda)$ by analyzing m_{ij} data obtained from both a two-dimensional Ising model and a mean-field Ising model. These models were simulated at various temperatures using the single-spin flip Metropolis dynamics.

In the first scenario, we considered square lattices with a linear dimension $L = 100$, resulting in a total of $N = 10000$ spins. We maintained the same number of spins in the second case. Our simulations employed $N_{MC} = 300$ and $N_{sample} = 100$, which is computationally highly efficient.

We repeated the process $N_{run} = 1000$ times to generate a sufficient number of eigenvalues for constructing histograms and calculating numerical moments:

$$\langle \lambda^k \rangle_{\text{numerical}} = \frac{\sum_{i=1}^{N_{bins}} \lambda_i^k \rho_{\text{numerical}}(\lambda_i)}{\sum_{i=1}^{N_{bins}} \rho_{\text{numerical}}(\lambda_i)}, \quad (10)$$

Our histograms were constructed with $N_{bins} = 100$. We anticipate that $\rho_{\text{numerical}}(\lambda)$ should approach $\rho(\lambda)$ according to Eq. 9 as $T \rightarrow \infty$ (in the paramagnetic phase). In this situation $\langle \lambda^k \rangle_{\text{numerical}}$ should closely align with theoretical value:

$$\langle \lambda^k \rangle = \int_{-\infty}^{\infty} \lambda^k \rho(\lambda) d\lambda = \sum_{j=0}^{k-1} \frac{\left(\frac{N_{sample}}{N_{MC}}\right)^j}{j+1} \binom{k}{j} \binom{k-1}{j}. \quad (11)$$

For $k = 1$, $\langle \lambda \rangle = 1$, and we expect $\langle \lambda \rangle_{\text{numerical}} \approx 1$ as $T \rightarrow \infty$. However for $T \approx T_C$ or $T < T_C$ the results warrant closer examination. We present the results for fluctuations in the Ising model, both in the two-dimensional and mean-field approximations, as functions of temperature, employing the parameters described above, as detailed in our previous observations [8, 9]. Figure 1 vividly illustrates that fluctuations exhibit a distinctive response concerning critical phenomena in the Ising model. This phenomenon holds true irrespective of whether we're considering Monte Carlo simulations in the two-dimensional Ising model or its mean-field approximation.

We can clearly discern a minimum point in the behavior of $\langle \lambda \rangle$ and an inflection point in $\langle \lambda^2 \rangle - \langle \lambda \rangle^2$ occurring precisely at $T = T_C$. As discussed in detail in [8, 9], this phenomenon is closely tied to the emergence of a gap when $T < T_C$, which subsequently closes as T approaches T_C . For a more comprehensive understanding, please refer to [8, 9], and also [10]. It is worth noting that $\langle \lambda \rangle_{\text{numerical}}$ approximates 1 for large values of T .

However, an intriguing question arises: How do $\langle \lambda \rangle$ and $\langle \lambda^2 \rangle - \langle \lambda \rangle^2$ behave when considering iterations of the Chirikov map instead of time-series data from spin systems? In the following section, we present the key findings of this study.

III. MAIN RESULTS

We conducted iterations of the Chirikov map, mirroring the approach employed in our study of the Ising model. In this case, we obtained matrix elements m_{ij} , which can now represent q_{ij} (iterations for position coordinates) or

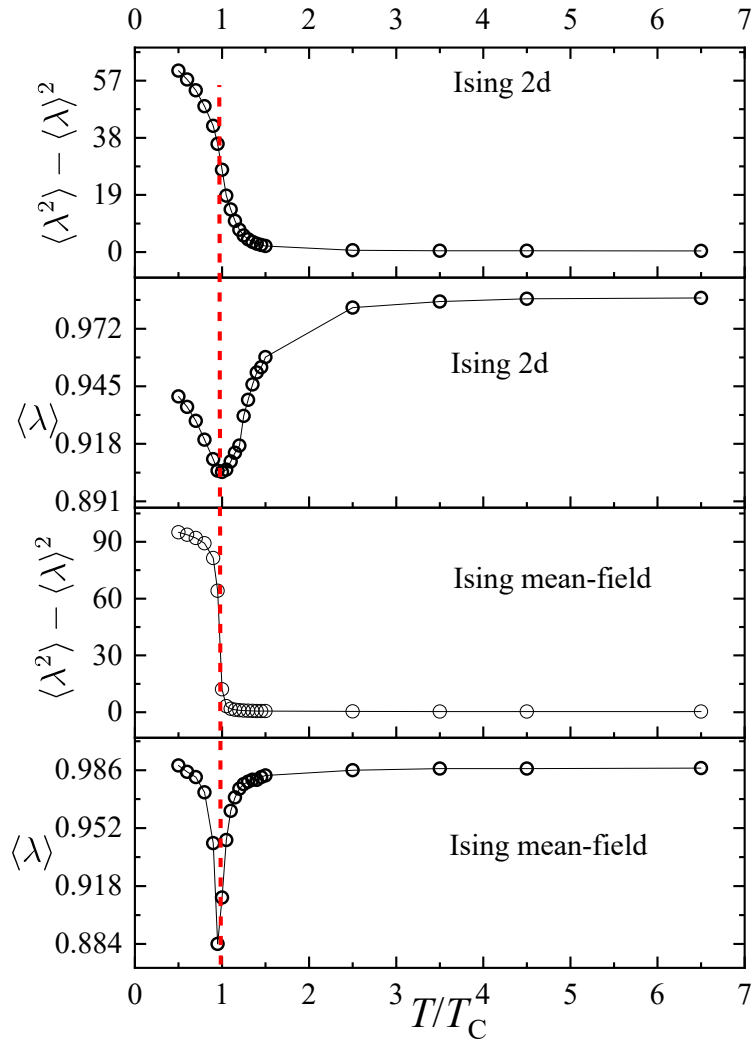


Figure 1. The fluctuations of eigenvalues in G were examined, taking into account the Ising model in two settings: a two-dimensional square lattice and a mean-field approximation, as reported in [8, 9]. Notably, we can discern a distinct peak occurring at $T = T_C$ for the average eigenvalue in both formulations of the Ising model. Additionally, an inflection point becomes apparent in the variance of the eigenvalue.

p_{ij} (iterations for moments). Here, $i = 1, \dots, N = 200$ iteration steps, and j ranges from 1 to $N_{sample} = 100$ different series. To initiate this process, we initialized random values for q_0 within the range $[0, 2\pi]$ and p_0 within the range $[0, 2\pi]$.

To provide a pedagogical visualization of the map iteration, let's consider a simple example. We observe the time evolutions q_i and p_i as functions of step $i = 1, 2, \dots, 100$ for three different initial conditions: $j = 1$ ($p_0 = 0.1$ and $q_0 = \pi$), $j = 2$ ($p_0 = 1$ and $q_0 = 1$), and $j = 3$ ($p_0 = \pi$ and $q_0 = 0.1$). These evolutions are presented in Figure 2, with the sequences displayed from bottom to top.

For the sake of illustration, we selected three distinct values of K . The first, $K = 0.971635$, signifies a scenario where the golden KAM curve is theoretically destroyed. The second, $K = \frac{\pi^2}{4}$, aligns with the Chirikov resonance-overlap criterion for defining the chaos border. Lastly, we considered $K = 10$, representing a situation characterized by complete and unbridled chaos.

To enhance the illustrative aspect, we also generated Poincaré sections corresponding to these three parameters, primarily for pedagogical purposes. To create these sections, we explored values for $(N_p + 1)(N_q + 1)$ different initial

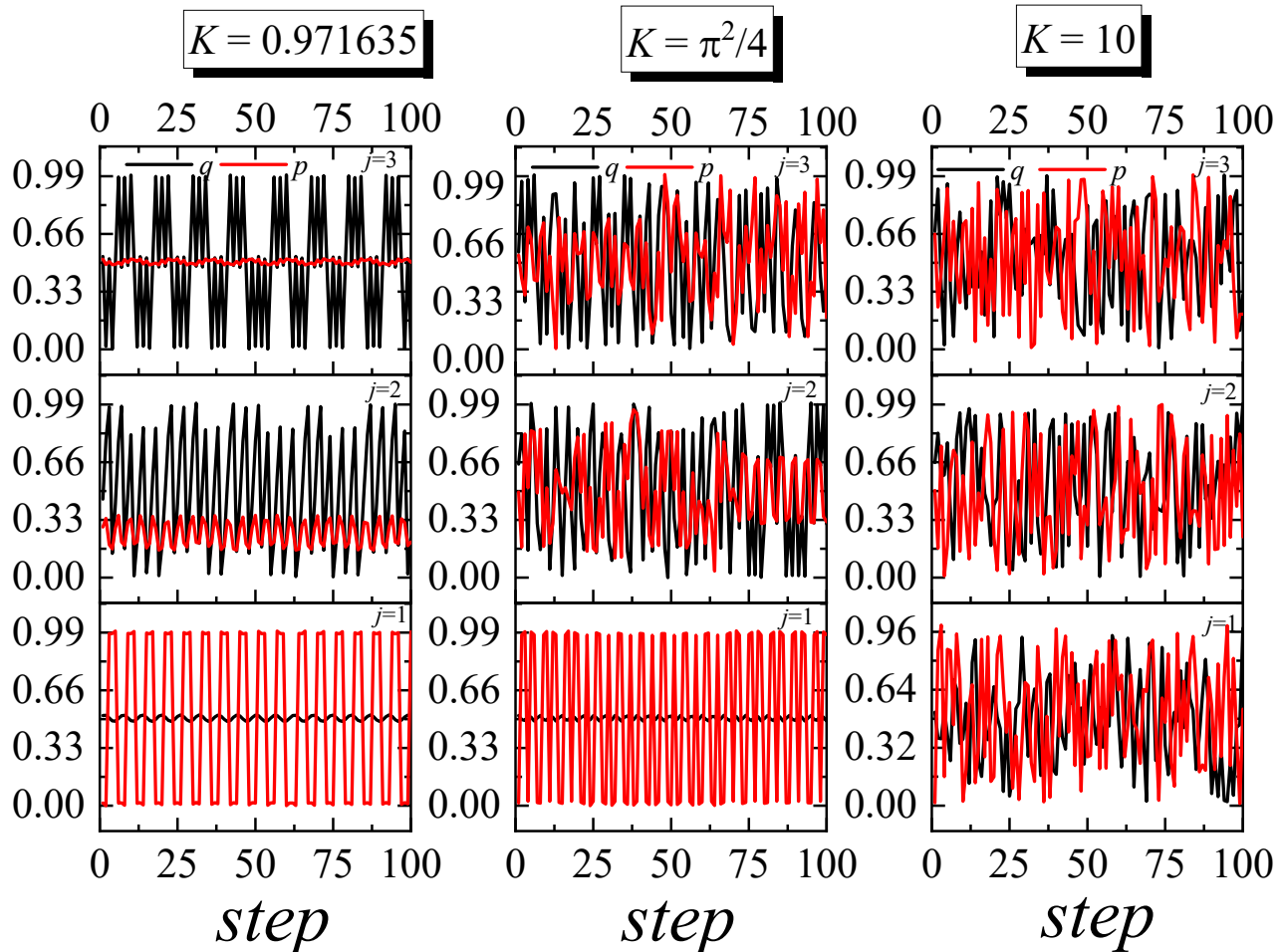


Figure 2. We engaged in iterations of moment and position coordinates within the framework of Chirikov’s map. The columns of matrix M were populated with N_{sample} iterations of position and moment pairs q_{ij}, p_{ij} . To illustrate this, we present a sample of time evolutions originating from three distinct initial conditions $(p_0, q_0) = (0.1, \pi), (1, \pi)$, and $(\pi, 0.1)$, respectively, displayed from bottom to top. These evolutions were examined under three different parameter values: $K = 0.971635$ (signifying the destruction of the golden KAM curve), $\frac{\pi^2}{4}$ (corresponding to the Chirikov criteria for the chaos border), and 10 (indicative of a state of complete chaos).

conditions parametrized as follows: $q_0 = \frac{2\pi}{N_q}l$ and $p_0 = \frac{2\pi}{N_p}m$, where $l = 0, 1, \dots, N_q$ and $m = 0, 1, \dots, N_p$. For effective visualization, we employed $N_q = N_p = n = 20$, resulting in q_0 and p_0 residing within the range $[0, 2\pi]$.

The intriguing and anticipated patterns can be vividly appreciated in Figure 3. Following this pedagogical exploration of the Chirikov method, we now proceed to utilize the random matrix method proposed here to shed light on the chaos border.

Our algorithm constructs an ensemble of matrices, comprising $N_{run} = 1000$ distinct matrices G of dimensions $N_{sample} \times N_{sample}$. These matrices correspond to N_{run} varying initial conditions, which are randomly selected with $q_0, p_0 \in [0, 2\pi]$. Subsequently, we diagonalize these matrices and organize the eigenvalues within the interval $\lambda_{min}^{(Numerical)}$ to $\lambda_{max}^{(Numerical)}$. We maintain a fixed number of bins, $N_{bin} = 100$, and generate histograms to calculate $\rho_{numerical}(\lambda_i)$.

We carried out this process for various values of K , ranging from $K_{min} = 0$ to $K_{max} = 10$. Consequently, we present the numerical density of eigenvalues for three distinct K values in Figure 4. In this figure, we display both the eigenvalues of G derived from the time evolutions of q and p . It’s noteworthy that for small values of K , a noticeable difference is observed when compared to the MP-law density, as described by equation 9. However, for $K = 10$, a substantial match between the numerical results and the theoretical prediction (MP-law, see Eq. 9) is evident. It’s important to note that this match is not perfect, which aligns with expectations since a perfect match would typically occur only for entirely random time series, not those displaying complete chaos.

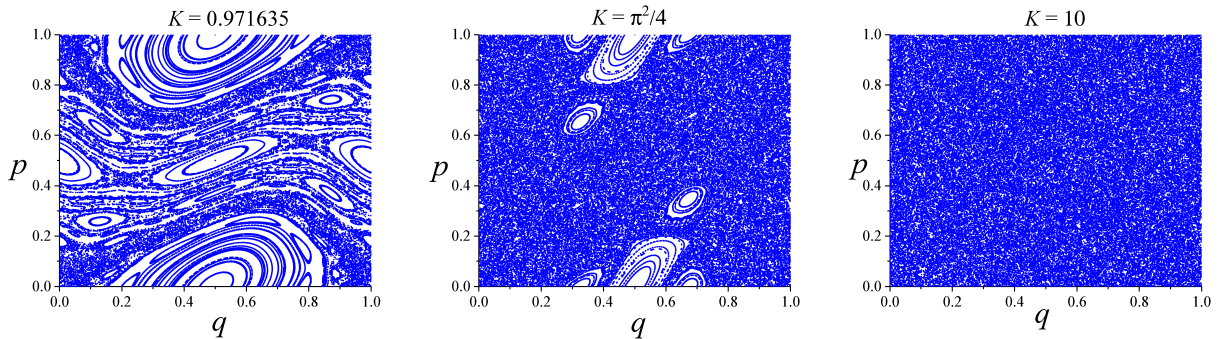


Figure 3. Poincaré sections were constructed for the same set of K values employed in Figure [?].

This suggests a potential approach for distinguishing chaos from random behavior, a crucial point as highlighted in [17]. Our exploration of random matrices holds promise in addressing this challenge, as underscored by parallel research efforts in [18].

In the context of spin systems (as discussed in [8–10]), we have observed a restoration of the Marchenko-Pastur law at elevated temperatures. While the system is predominantly stochastic rather than highly chaotic in this scenario, we can draw a meaningful analogy. To further investigate this phenomenon, we examine the fluctuations of eigenvalues, as described in Equation 10, particularly those derived from time-evolutions of moments.

These results are visually depicted in Figure 5. It is quite intriguing to decipher the insights conveyed by this plot. In Figure 5 (a), the fluctuations in the average eigenvalue are displayed as a function of K for 10 different seeds. Notably, the outcomes exhibit minimal variation across different seeds. Figure 5 (b) presents the same plot along with error bars for added clarity.

We observe that the global minimum, denoted by the green dashed line, precisely occurs at $K \approx 2.46$, not by coincidence. This numerical value aligns with $\pi^2/4$, which corresponds to the Chirikov resonance-overlap criterion for the border of chaos. This same pattern emerges in the dispersion of eigenvalues, as depicted in both Figure 5 (c) and Figure 5 (d). The former illustrates the variance among different seeds, while the latter shows the averaged under these seeds. Remarkably, $K \approx 2.46$ also serves as the global minimum for the dispersion of eigenvalues.

The value $K \approx 2.46$ surpasses the baseline $K = 0.9716$ for several reasons, including the influence of secondary-order resonances and the finite width of the chaotic layer, as well as findings observed by [19]. Interestingly, these authors note that such effects on the Chirikov map appear to be less pronounced.

Furthermore, it is worth noting that $K = 0.9716$, indicated by the dashed magenta line in the same plot, anticipates a significant upturn in both behaviors, specifically in $\langle \lambda \rangle \times K$ and $\langle \lambda^2 \rangle - \langle \lambda \rangle^2 \times K$. This trend seems to exhibit universality. Lichtenberg and Lieberman [1] have proposed a refinement of K as $K = \frac{\pi^2}{4}$, which would suggest $K \approx 1.2$. This refinement is represented by the yellow dashed line in Figure 5. It is evident that this point consistently demonstrates an increase after the critical $K = 0.9716$.

To provide a comprehensive view, we also examine the eigenvalues associated with the time evolutions of positions. Interestingly, we continue to observe the global minimum occurring at approximately $K \approx 2.46$, aligning with the Chirikov resonance-overlap criterion for the chaos boundary. This pattern appears to exhibit universality. However, a noteworthy departure arises when considering the eigenvalue dispersion, as we now observe a global maximum at the same K value. This intriguing phenomenon is depicted in Figure 6. To maintain consistency, we employ a similar approach to illustrate the points $K = 0.9716$ and $K \approx 1.2$.

IV. CONCLUSIONS

In our study, we utilize the technique of Wishart-like matrix spectra fluctuations to probe the existence of chaos within Chirikov’s standard map. This methodology draws inspiration from its past success in characterizing critical points within spin systems. Our results consistently affirm that the resonance-overlap criterion for the chaos boundary, denoted as $K = \left(\frac{\pi}{4}\right)^2 \approx 2.46$, holds true whether we examine the spectra obtained from the evolutions of moments or from the evolutions of position coordinates.

However, intriguingly, when it comes to the dispersion, $\langle \lambda^2 \rangle - \langle \lambda \rangle^2$, this same K value remains a global minimum for the evolutions of moments but transforms into a global maximum for the evolutions of positions.

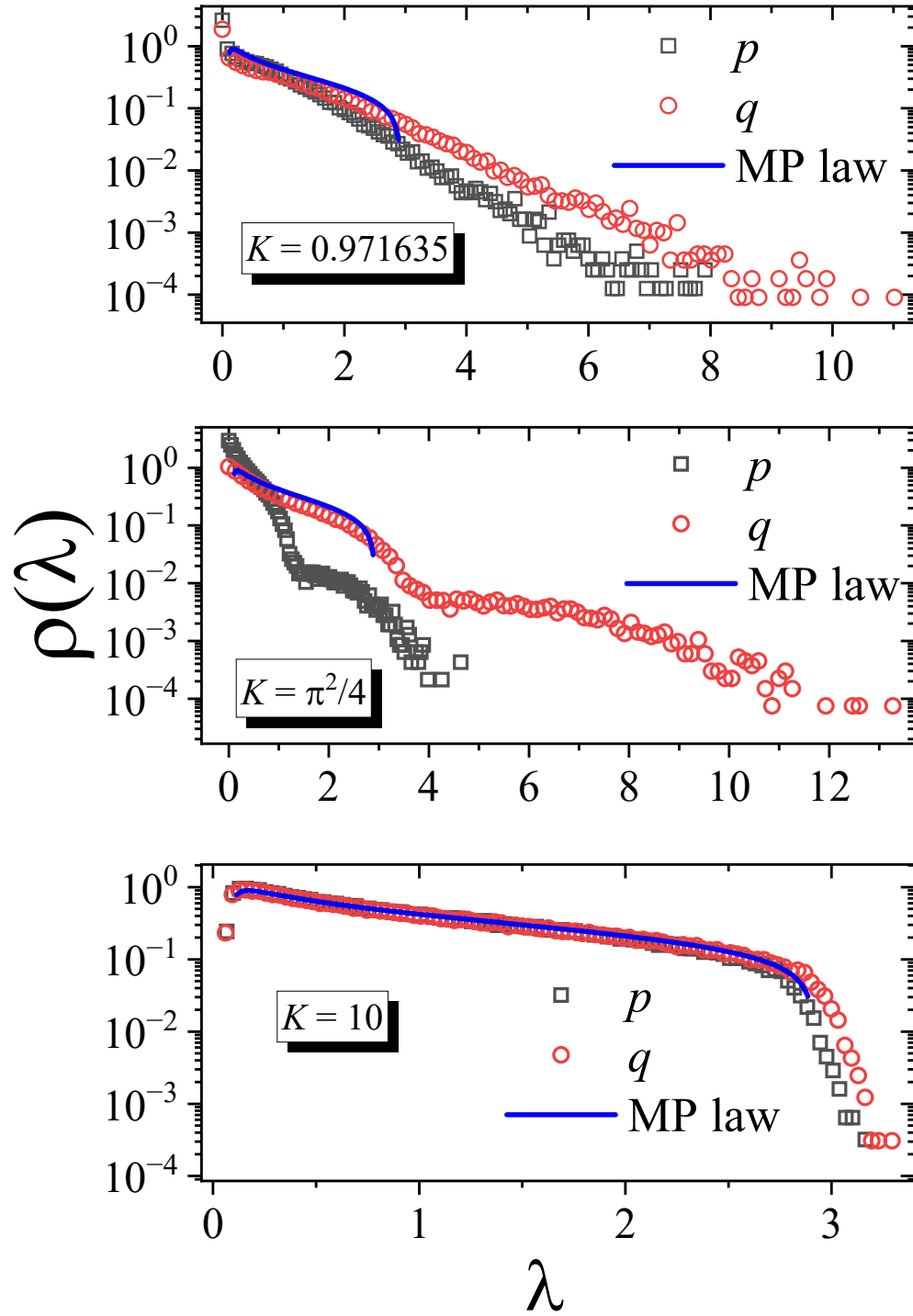


Figure 4. The density of eigenvalues for various K values is depicted here. In the chaotic regime, we can discern a notable alignment with the MP-law, indicating a good fit.

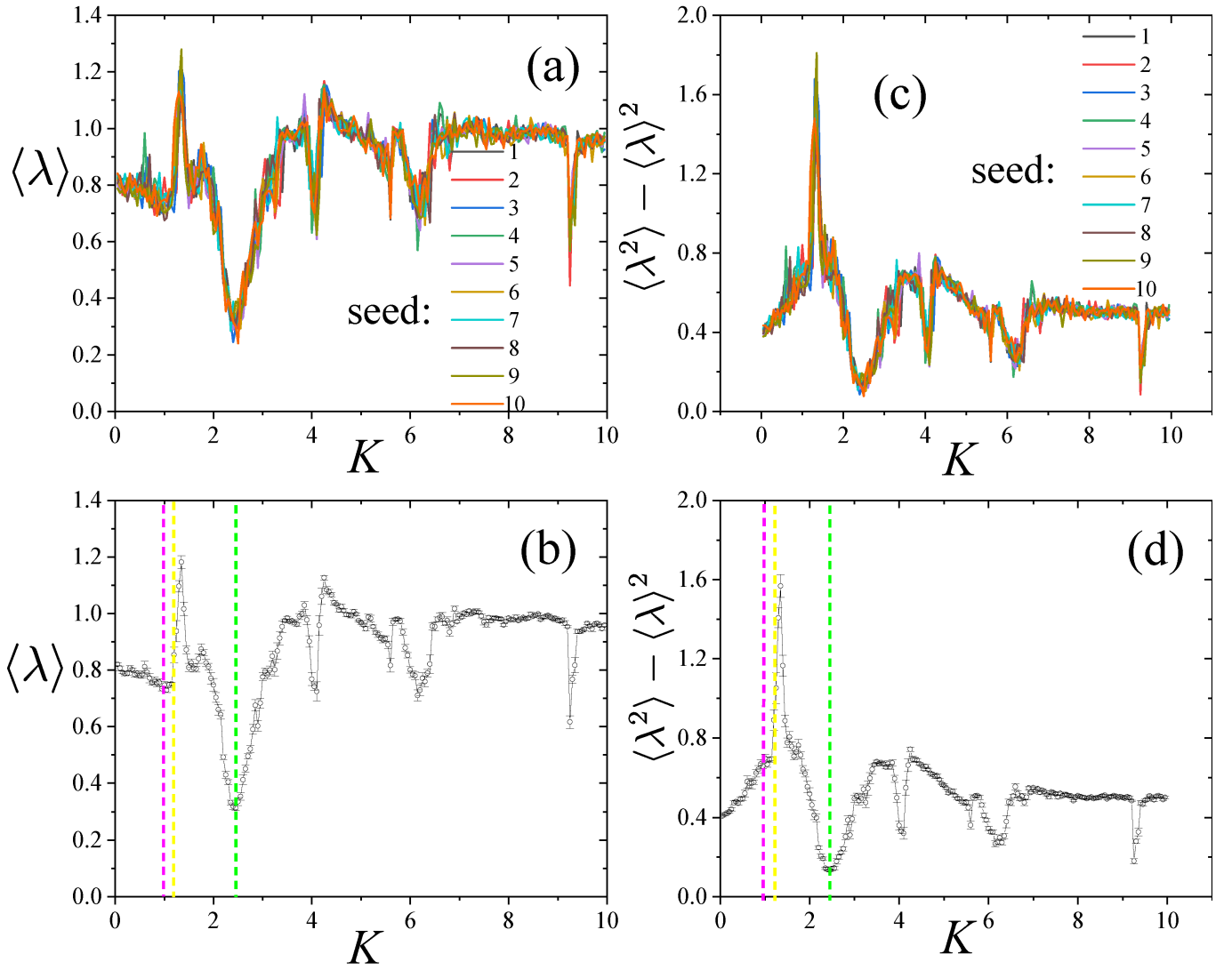


Figure 5. Fluctuations in the eigenvalues of the matrix G are investigated by constructing it through the time evolutions of p .

Furthermore, the value $K = 0.971635$, which marks the point at which the golden KAM curve is disrupted, appears to foreshadow extreme behaviors in eigenvalue fluctuations. This study holds promise in unraveling the intricate relationship between chaos and quantum mechanics, but it merits further exploration and extension to other models. Such analyses could prove invaluable in enhancing our understanding of this complex interplay.

-
- [1] A. J. Lichtenberg, M. A. Leiberman, Regular and chaotic dynamics, Springer (1992)
[2] R. da Silva, D. E. Peretti, S. D. Prado, Appl. Math. Model. **40**, 10689 (2016)
[3] R. da Silva, S. D. Prado, H. A. Fernandes, Commun. Nonlinear Sci. Numer. Simul. **51**, 105 (2017)
[4] E. P. Wigner, Ann. Math. **53**, 36 (1951)
[5] E. P. Wigner, Ann. Math. **62**, 548 (1955)
[6] F.J. Dyson, J. Math. Phys. **3**, 140–156, 157–165, 166–175 (1962)
[7] J. Wishart, Biometrika **20A**, 32 (1928)
[8] R. da Silva, Int. J. Mod. Phys. C **34**, 2350061 (2023)
[9] R. da Silva, E. Venites, S. D. Prado, J. R. Drugowich de Felício, ArXiv. <https://doi.org/10.48550/arXiv.2302.07990> (2023)
[10] R. da Silva, H. C. M. Fernandes, E. Venites Filho, Sandra D. Prado, J. R. Drugowich de Felício, Braz. J. Phys. **53**, 80

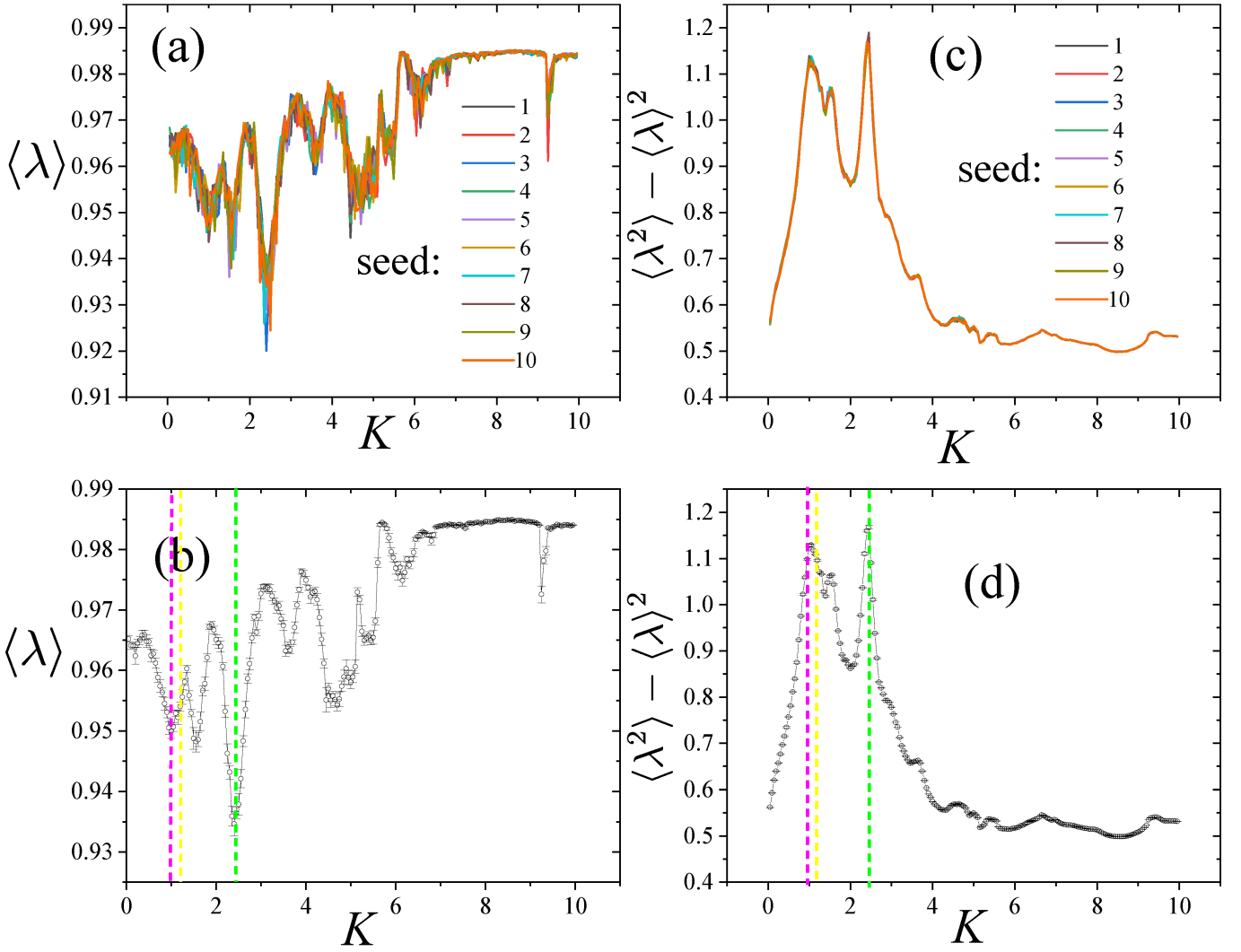


Figure 6. The fluctuations in the eigenvalues of the matrix G , which is constructed through iterations of x , are under examination.

(2023)

- [11] V. A. Marcenko, L. A. Pastur, Math. USSR Sb. **1** 457 (1967)
- [12] B.V.Chirikov, Phys. Rep. **52**, 263 (1979)
- [13] M. L. Mehta, Random Matrices, Academic Press, Boston (1991)
- [14] Y. Sinai, A. Soshnikov, Bol. Soc. Bras. Mat. **29**, 1 (1998)
- [15] T. Guhr, A. Muller-Groeling, H. A. Weidenmuller, Phys. Rep. **299**, 189 (1998)
- [16] Vinayak, T. H. Seligman, AIP Conf. Proc. **1575**, 196 (2014)
- [17] B. R. R. Boaretto, R. C. Budzinski, K. L. Rossi, T. L. Prado, S. R. Lopes, C. Masoller, Sci. Rep. **11**:15789 (2021)
- [18] We are currently engaged in research centered around the utilization of random matrices as a tool for distinguishing between random processes and chaotic behaviors. This research is currently in the preparatory phase.
- [19] K. M. Frahm, D. L. Shepelyansky Phys. Rev. E **80**, 016210 (2009)